Modeling of measurement condenser microphones at low frequencies: numerical issues

Cutanda Henriquez, Vicente; Juhl, Peter Møller; Barrera Figueroa, Salvador

Published in:
Proceedings of internoise 2019

Publication date:
2019

Document Version
Publisher's PDF, also known as Version of record

MADRID
inter.noise 2019
June 16 - 19
NOISE CONTROL FOR A BETTER ENVIRONMENT

Modeling of measurement condenser microphones at low frequencies: numerical issues

Cutanda Henríquez, Vicente[1]
Centre for Acoustic-Mechanical Micro Systems, Technical University of Denmark
Ørsteds Plads, Building 352, DK-2800, Kgs. Lyngby, Denmark

Juhl, Peter Møller[2]
University of Southern Denmark, Electrical Engineering
Campusvej 55, DK-5230 Odense M, Denmark

Barrera Figueroa, Salvador[3]
Danish Fundamental Metrology A/S
Kogle Allé 5, DK-2970 Hørsholm, Denmark

ABSTRACT

Numerical modeling of condenser microphones is a challenging task. In these devices, there is a strong coupling between the exterior medium, the metallic stretched membrane, and the interior domain. Viscous and thermal losses in the narrow gap between membrane and back plate play a central role in the precise damping of the membrane's first resonance and the definition of the sensitivity at high frequencies. The inclusion of losses means a drastic increase in the computational load and makes the modeling of the most complicated units very cumbersome. The difficulty is even higher when whole calibration systems, such as primary reciprocity setups, need to be modeled. There is a need for such models from the metrological community. In previous publications, the Boundary Element Method (BEM) has shown to be able to model several measurement condenser microphones, some of them containing many holes in the backplate. There is, however, a difficulty when low frequencies are modeled. The limit for "low" frequency depends on the unit, but it is generally below the membrane resonance. This issue is the consequence of the instability of the BEM at low frequencies for interior domains, where the pressure in the cavity is almost uniform. Some solutions have been found for microphone models that minimize this effect, but a complete removal would be more desirable. In this paper, the issue will be examined from the practical point of view. Some new remedies will be proposed, including numerical approaches that preserve the advantages of the BEM and can become more stable in the referred cases.

Keywords: Microphones, Boundary Element Method, Visco-thermal losses
I-INCE Classification of Subject Number: 71, 76

[1] vche@elektro.dtu.dk
[2] pmjuhl@mci.sdu.dk
[3] sbf@dfm.dk

1. INTRODUCTION

Condenser microphones are reliable and stable devices with outstanding performance. They offer a wide frequency range, low noise, long-term stability and low distortion. These properties make them suitable for high-end audio applications and acoustic measurements. Their transduction principle relies on the charge variations induced in the capacitor formed by a stretched metallic diaphragm, exposed to the sound field, and a very close back electrode. The thickness of the gap between electrodes is just a few micrometers, and determines not only the sensitivity of the transducer but also the damping, through viscous and thermal losses, of the diaphragm resonance. The device is therefore a strongly coupled combination of the electrical capacitor, interior cavity, gap region, diaphragm and external domain.

The creation of numerical models of condenser microphones involves some specific challenges: i) the aspect ratio of the microphone dimensions is very large, so that the model has to deal with a very thin gap and other much larger domains, ii) viscous and thermal losses in the gap are very relevant and need to be modeled accurately, and iii) verification of microphone models is conditioned by the uncertainty of their internal parameters: the measured sensitivity significantly varies, even among units of the same model, due to the fabrication tolerances.

Numerical modeling of condenser microphones has been done using the full Finite Element Mothod (FEM) [1, 2]. The Boundary Element Method (BEM) with visco-thermal losses [3, 4] has as well been employed on microphones [5, 6]. The present paper focuses on the BEM, which has some advantages over other modeling approaches, such as computational load for large setups, but also presents some specific challenges that have to do with the instability of the BEM for interior problems at low frequencies [7, 8]. The BEM models of microphones presented in [5, 6] show, if untreated, an excess in the acoustic pressure in the back cavity of the microphone at frequencies low enough for this pressure to be uniform, leading to a reduced movement of the membrane and lower sensitivity. This instability has been reduced in [5, 6] by creating a small region with finite impedance in the interior of the back cavity, emulating the existence of a vent hole, a common feature in condenser microphones. In the present work, we investigate the limits for this instability by means of a new numerical implementation with visco-thermal losses where a combination of the FEM and the BEM is used.

The rest of this paper is distributed as follows: i) the so-called low-frequency problem is discussed in section two, ii) the numerical models, and in particular the FEM-BEM formulation, are described and commented in section three, iii) in section four, two numerical examples, a simplified microphone with no back cavity and a Brüel & Kjaer type 4938 microphone, are modeled with the proposed formulation , and iv) the results are commented and conclusions drawn in the final section five.

2. THE LOW-FREQUENCY PROBLEM

Any interior domain shows, as the frequency is reduced and under an acoustic excitation, a sound pressure that is nearly uniform. Such a domain could then be described as a simple acoustic compliance and, for a known excitation, the value of the uniform pressure can thus be obtained. A numerical method, however, aims at obtaining a piecewise solution and naturally shows ill-conditioning for low-frequency

closed domains. This phenomenon has been shown by some authors regarding the BEM, but it is not otherwise often touched upon in the literature [7, 8]. The BEM is most commonly used for exterior domain applications, and in this case the Sommerfield radiation condition, which ensures that the pressure is zero at an infinite distance, effectively stabilizes the solution. The fundamentals of this issue are examined further in this conference in a contribution by the same authors of this paper.

A measurement condenser microphone is essentially a cavity that is closed by the sensing membrane and only connected to the exterior by a small pressure equalization vent. The vent has only an effect at very low frequencies, usually below the audible frequency range. Microphone models using BEM with losses show a drift in the calculated sensitivity as the frequency decreases. The method used in [5, 6] to alleviate this effect is described in [9] and consists on assigning a non-infinite impedance to one of the BEM nodes in the back cavity. The impedance is made to resemble that of an actual microphone vent. The result is satisfactory, but it is however a remedy that does not remove the essential instability of the BEM in cavities at low frequencies.

Further improvements in the BEM implementation with losses aim at avoiding the use of finite difference derivatives [10,11]. However, these improvements, again, cannot avoid the fundamental issue described here. The examples and developments in this paper will be based in the 'original' BEM with losses as described in [3, 4].

3. NUMERICAL MODELS

In this section, the BEM formulation and its application for coping with viscothermal losses are briefly described. This formulation is then modified so as to introduce the use of FEM on the propagating acoustic 'mode', while maintaining the BEM calculation of the lossy viscous and thermal contributions. The initial purpose of this FEM-BEM implementation is trying to answer the questions: i) is the BEM causing the low frequency issue alone?, ii) is FEM more robust for dealing with closed cavities when losses are modeled on the boundary? Besides the study of the low-frequency behavior, the FEM-BEM formulation is in its own right a new option for modeling visco-thermal losses.

3.1. The BEM with visco-themal losses

The classical BEM implementation in acoustics starts with the Helmholtz Integral Equation (HIE), which is derived from the harmonic wave equation. The $e^{i\omega t}$ harmonic time dependence convention is used.

$$C(P)p(P) = \int_S \left[\frac{\partial G(Q)}{\partial n} p(Q) - \frac{\partial p(Q)}{\partial n} G(Q)\right] dS + p^I(P) \tag{1}$$

In Eq. (1), p is the sound pressure, G is the Green's function and P and Q are points in the domain and on the surface respectively. $C(P)$ is a geometrical constant and $p^I(P)$ is the incident pressure, if present. In the direct collocation version of BEM employed here [12], point P is *collocated*, one at a time, on all nodes (Q points) of a mesh defined over the domain boundary, thus creating a system of equations which can be solved, given a set of boundary conditions, on the boundary [13].

$$\mathbf{Ap} - \mathbf{B}\frac{\partial \mathbf{p}}{\partial n} + \mathbf{p^I} = 0 \tag{2}$$

The coefficient matrices **A** and **B** in Eq. (2) are the result of the integration over the boundary mesh of of Eq. (1) using collocation. Having obtained the acoustic variables on the domain boundary, it is straightforward to obtain their values on any domain point by reapplying the discretized version of Eq. (1) with no collocation.

The finite difference-based version of BEM with losses (abbreviated as FDD-BEM) takes its starting point on the Kirchhoff decomposition of the Navier-Stokes equations, [14, 15]

$$(\Delta + k_a^2)p_a = 0 \tag{3}$$

$$(\Delta + k_h^2)p_h = 0 \tag{4}$$

$$(\Delta + k_v^2)\vec{v}_v = \vec{0}\ , \text{with}\ \ \nabla \cdot \vec{v}_v = 0 \tag{5}$$

The Kirchhoff decomposition consists of three so-called *modes*: acoustic (denoted with the a subscript), thermal (h subscript) and viscous (v subscript). The three modes are defined in the three independent equations (3-5), with Eq. (5) being a vectorial equation that can can be split into three scalar components when dealing with a three-dimensional domain. The incident pressure term in Eqs. (1,2) has been removed for this analysis. The three modes are coupled by a set of conditions on the boundary,

$$T = T_a + T_h = \tau_a p_a + \tau_h p_h = 0 \tag{6}$$

$$\vec{v}_{boundary} = \phi_a \nabla p_a + \phi_h \nabla p_h + \vec{v}_v \tag{7}$$

where the total sound pressure is $p = p_a + p_h$ (no viscous pressure) and the total particle velocity vector is $\vec{v} = \vec{v}_a + \vec{v}_h + \vec{v}_v$. The three wavenumbers k_a, k_h and k_v and the parameters τ_a, τ_h, ϕ_a and ϕ_h are function of the lossless wavenumber and the physical properties of the fluid: viscosity and thermal conductivity coefficients, air density, and specific heats. Eqs. (6,7) mean respectively that: i) the temperature T does not vary directly over the boundary, due to the very different thermal conductivities of the fluid and the boundary material, and ii) fluid particles cannot move tangentially over the boundary, the so-called *no-slip* condition. Note that Eqs. (3-5) are formally equivalent to the Helmholtz equation $(\Delta + k^2)p = 0$, and can be reformulated in the integral form of Eq. (1) and further discretized using BEM as

$$\mathbf{A}_a \mathbf{p}_a - \mathbf{B}_a \frac{\partial \mathbf{p}_a}{\partial n} = 0 \tag{8}$$

$$\mathbf{A}_h \mathbf{p}_h - \mathbf{B}_h \frac{\partial \mathbf{p}_h}{\partial n} = 0 \tag{9}$$

$$\mathbf{A}_v \vec{\mathbf{v}}_v - \mathbf{B}_v \frac{\partial \vec{\mathbf{v}}_v}{\partial n} = \vec{0}\ , \text{with}\ \ \nabla \cdot \vec{\mathbf{v}}_v = 0 \tag{10}$$

where the coefficient matrices ($\mathbf{A}_a$, $\mathbf{B}_a$, $\mathbf{A}_h$, $\mathbf{B}_h$, $\mathbf{A}_v$, $\mathbf{B}_v$) are obtained through the collocation method, in the same way as matrices ($\mathbf{A}, \mathbf{B}$) in Eq. (2). The full derivation starts with the normal component of the discretized version of Eq. (7)

$$\mathbf{v}_{boundary,n} = \phi_a \mathbf{B}_a^{-1} \mathbf{A}_a\ \mathbf{p}_a - \phi_h \mathbf{B}_h^{-1} \mathbf{A}_h \frac{\tau_a}{\tau_h}\ \mathbf{p}_a + \mathbf{v}_{v,n} \tag{11}$$

The remaining of the derivation in Ref. [4] is dedicated to obtaining an expression of $\mathbf{v}_{v,n}$, the normal component of the viscous velocity, which is a function of the viscous

coefficient matrices $\mathbf{A}_v$ and $\mathbf{B}_v$, the boundary condition for the tangential velocity and the acoustic pressure $\mathbf{p}_a$. This derivation will not be repeated here. It leads to a system of equations of the form $\mathbf{C}_{BEM}\mathbf{p}_a = \mathbf{v}_{boundary}$, if no incident pressure and no tangential movement of the boundary are assumed, as is the case for the examples presented here. The matrix $\mathbf{C}_{BEM}$ is the coefficient matrix of the full BEM with losses.

3.2. The FEM-BEM with visco-themal losses

In order to construct the FEM-BEM formulation with losses, the BEM described above is combined with a FEM model of the interior domain. The FEM model is implemented using the MATLAB PDE toolbox. The FEM system of equations for the harmonic wave equation has the form

$$(-\mathbf{K} + k^2\mathbf{M})\,\mathbf{p} = \mathbf{F} \tag{12}$$

where the force term $\mathbf{F}$ contains the boundary condition and $\mathbf{K}$ and $\mathbf{M}$ are the stiffness and mass matrices. The FEM is applied on the acoustic mode arising from the Kirchhoff decomposition, in Eq. (8). The lossless wavenumber k is replaced by the acoustic mode wavenumber k_a and the whole domain is meshed. The BEM mesh is then obtained as the corresponding boundary mesh matching the FEM domain mesh. The FEM system of equations can be rewritten as

$$(-\mathbf{K} + k^2\mathbf{M})\,\mathbf{p}_a = \mathbf{RHS}\,\mathbf{v}_{a,n} \tag{13}$$

where the force term $\mathbf{F}$ has been replaced by a right-hand-side matrix times the acoustic part of the normal boundary velocity. Since Eq. (11) represents the normal velocity component of the sum of mode contributions $\mathbf{v}_{boundary,n} = \mathbf{v}_{a,n} + \mathbf{v}_{h,n} + \mathbf{v}_{v,n}$, equations (11) and (13) can be combined as

$$(-\mathbf{K} + k^2\mathbf{M})\,\mathbf{p}_a = \mathbf{RHS}\,(\mathbf{v}_{boundary,n} + \phi_h\mathbf{B}_h^{-1}\mathbf{A}_h\frac{\tau_a}{\tau_h}\,\mathbf{p}_a - \mathbf{v}_{v,n}) \tag{14}$$

where the BEM matrices, velocities and pressures have been expanded to the size of the FEM system of equations. This expansion is done by assigning the BEM coefficients to the nodes of the FEM mesh that are on the boundary and make up the BEM mesh. Eq. (14) can be now used on an interior radiation problem for obtaining the unknown $\mathbf{p}_a$. in the domain, and therefore also on the boundary. The boundary $\mathbf{p}_a$ solution leads to all remaining magnitudes of the problem with visco-thermal losses on the boundary and the domain, as described in Ref. [4]. We can write Eq. (14) in a simplified form as $\mathbf{C}_{FEM-BEM}\,\mathbf{p}_a = \mathbf{RHS}\,\mathbf{v}_{boundary}$, where $\mathbf{C}_{FEM-BEM}$ contains the contributions fron the FEM coefficient matrices and the viscous and thermal parts of the BEM implementation.

Note that the viscous and thermal BEM coefficient matrices ($\mathbf{A}_h$, $\mathbf{B}_h$, $\mathbf{A}_v$, $\mathbf{B}_v$) are sparse matrices due to the heavy losses: the effect of most of the geometry on a given collocation point is negligible except for the closest regions. The FEM part is also represented by a matrix with most coefficients on the diagonal. Moreover, even though the FEM-BEM needs a domain mesh rather than a boundary mesh, one does not need to mesh the boundary layers finely as it is done in the FEM with losses, since they are taken into account by the BEM components. The FEM-BEM can therefore benefit from sparse solvers very much like the FEM with no losses, whith the only overhead of the calculation of the non-zero coefficients of ($\mathbf{A}_h$, $\mathbf{B}_h$, $\mathbf{A}_v$, $\mathbf{B}_v$).

3.3. Coupling with a microphone membrane

In a condenser microphone, the interior domain, the membrane and the exterior domain are coupled [5]. The exterior domain is replaced by an uniform excitation in this paper without loss of generality, since the exterior domain does not affect the examined issues in the interior. Such uniform excitation corresponds experimentally to an electrostatic actuator. The membrane is assumed with no stiffness and its equation is

$$\frac{\partial^2 \epsilon}{\partial r^2} + \frac{1}{r}\frac{\partial \epsilon}{\partial r} + K^2\,\epsilon = \frac{p_{diff}}{T} \tag{15}$$

where ϵ is the normal displacement, r is the radial coordinate and $K = \omega(\frac{\sigma}{T})^{1/2}$ is the membrane's wavenumber, with ω the acoustic angular frequency, σ the surface density and T the membrane tension. Note that the membrane is assumed circular with no variations in the circumferential direction. p_{diff} is the difference of acoustic pressures on both sides of the membrane. The membrane is modeled using FEM, obtaining the system of equations

$$T(\mathbf{A}_m + K^2\mathbf{B}_m)\,\boldsymbol{\epsilon} = \mathbf{p}_{diff} \tag{16}$$

where $\mathbf{A}_m$ and $\mathbf{B}_m$ are the stiffness and mass matrices of the membrane model. The membrane can be coupled to the interior domain of the microphone by

$$\begin{bmatrix} T(\mathbf{A}_m + K^2\mathbf{B}_m) & \mathbf{D} \\ -i\,\omega & \mathbf{C}_{BEM} \end{bmatrix} \begin{Bmatrix} \epsilon_i \\ \mathbf{p}_{a,i} \end{Bmatrix} = \begin{Bmatrix} \mathbf{p}_{inc} \\ 0 \end{Bmatrix} \tag{17}$$

$$\begin{bmatrix} T(\mathbf{A}_m + K^2\mathbf{B}_m) & \mathbf{D} \\ -i\,\omega\,\mathbf{RHS} & \mathbf{C}_{FEM-BEM} \end{bmatrix} \begin{Bmatrix} \epsilon_i \\ \mathbf{p}_{a,i} \end{Bmatrix} = \begin{Bmatrix} \mathbf{p}_{inc} \\ 0 \end{Bmatrix} \tag{18}$$

where D is a coupling matrix providing the interior pressure excitation to the membrane and $-i\,\omega$ couples the membrane velocity to the interior. The incident uniform pressure $\mathbf{p}_{inc}$ is the external membrane excitation. Equations (17) and (18) correspond respectively to the interior domain modeled with BEM or with FEM-BEM respectively.

3.4. Axisymmetrical implementation

The examples in this paper are fully axisymmetrical and are modeled with fully axisymmetrical versions of the BEM and FEM-BEM [3, 13]. There is no loss of generality: the axisymmetrical microphone models show the same low-frequency issues than the fully three-dimensional ones, while they are more convenient for the analysis.

4. SIMPLE MICROPHONE MODEL WITHOUT BACK CAVITY

The first example is a simplified condenser microphone model consisting only on a circular membrane clamped at its edge, and a close back plate electrode of the same size. The membrane is excited with a uniform pressure of 1 Pa and the pressure is assumed zero at the rim. The geometry and the BEM and FEM meshes are represented in Figure 1. The FEM domain mesh is calculated first and the BEM mesh is obtained from the FEM nodes on the boundary. For all examples shown in this paper, the BEM mesh uses three-node quadratic line elements and the FEM mesh uses six-node quadratic triangular elements.

This setup has an analytical solution in [16], which has been used in several other publications [3,5] as a reference test case. The BEM mesh has 91 nodes and 45 elements, and the FEM mesh has 155 nodes and 52 elements. The distance between membrane and back electrode is 18 μm and the radius is 2 mm. The diaphragm tension is 3128 N/m, the density of the diaphragm material is 8300 kg/m^3, and the diaphragm thickness is 6.95 μm.

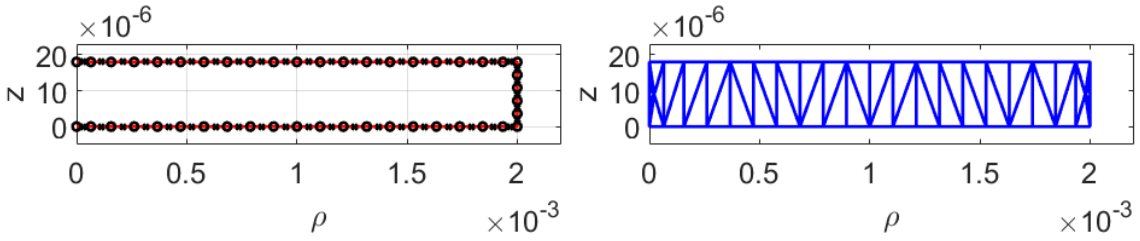

Figure 1: Generator and meshes of the axisymmetrical geometry of the simple microphone. Left: BEM mesh; right: FEM mesh. The top circular lid represents the membrane, excited by a uniform pressure. The rim has a $p = 0$ boundary condition and the bottom lid is a hard back plate ($v = 0$). Note the different scales of the axes.

Figure 2 shows the averaged pressure acting on the back of the membrane, inside the gap between electrodes, as a function of frequency. The FEM-BEM formulation is closer to the analytical solution, but both BEM and FEM-BEM increase their error as the frequency decreases.

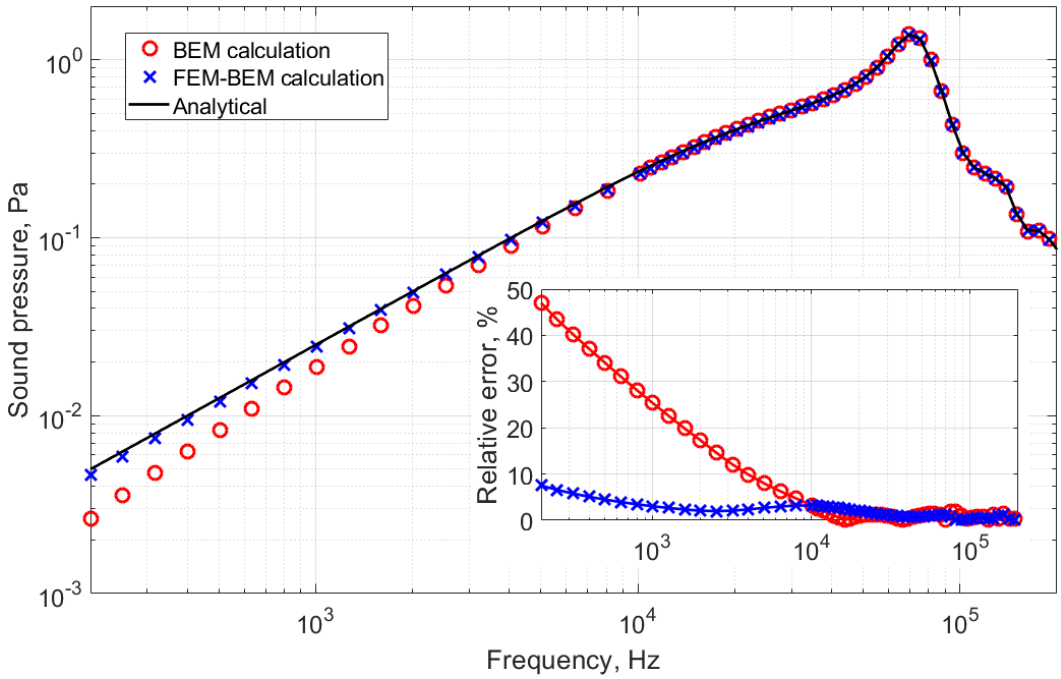

Figure 2: Averaged sound pressure modulus behind the membrane of the simple microphone. Circles: BEM-only calculation; crosses: FEM-BEM calculation; solid line: analytical solution from [16]. Inset: relative errors of the BEM and FEM-BEM solutions.

The averaged membrane displacement, as calculated with the FEM-BEM, is closer to the analytical solution, as shown in Figure 3. The two numerical solutions, however, are both quite close to the analytical solution.

From this example, one can conclude that the FEM-BEM formulation brings an improvement to the calculation of this interior problem with losses, at the cost of having to mesh the whole domain.

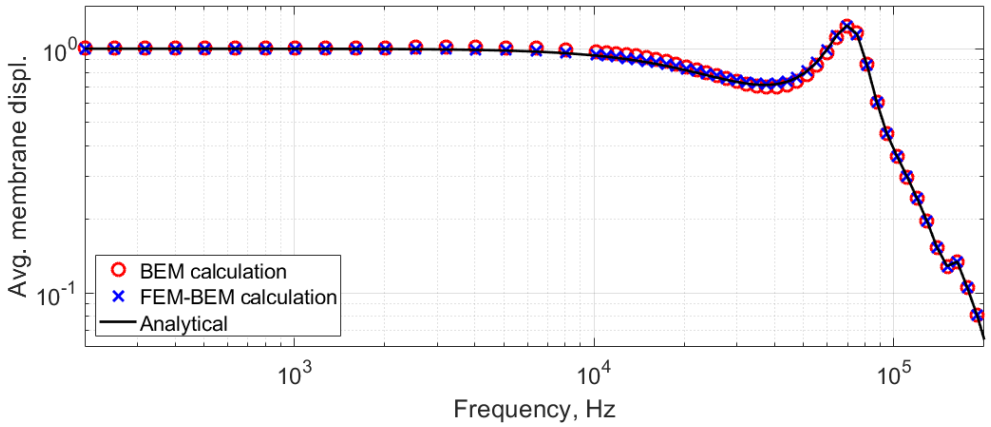

Figure 3: Averaged displacement of the membrane of the simple microphone. Circles: BEM-only calculation; crosses: FEM-BEM calculation; solid line: analytical solution from [16]. All curves are normalized with the analytical displacement at 200 Hz.

5. MODEL OF A MICROPHONE WITH BACK CAVITY

The second example is a Brüel & Kjær type 4938 1/4″ pressure-field condenser microphone. This microphone does not have any hole in the backplate, making it suitable for modeling as rotationally symmetrical. In this case there is no analytical solution to compare with. There are measurements of the sensitivity of this type of microphone made with an electrostatic actuator, which provides the uniform pressure excitation used in the models. However, no two units of a microphone model are alike due to fabrication tolerances. For this reason, a group of measurements of 183 units of the Brüel & Kjær 4938 is used to produce upper and lower limits. These measurement results have previously been used in [9].

In order to complete the picture, a version of the microphone with no closed back cavity has also been simulated using BEM with visco-thermal losses. The dimensions of the membrane, gap and backplate, as well as the tension and density of the membrane, are the same as in the Brüel & Kjær 4938. When excited with a uniform pressure, this open setup should give a very similar sensitivity to that of a closed microphone, but, lacking a back cavity, it would not be affected by the low frequency issue outlined in section 2. The thickness of the gap is in all three cases 19,8 μm, the radius of the membrane is 2 mm and the radius of the back plate is 1,75 mm. The diaphragm tension is 3128 N/m, the density of the diaphragm material is 8300 kg/m^3, and the diaphragm thickness is 6.95 μm.

Figure 4 shows the geometry and meshes of both the Brüel & Kjær 4938 and its open counterpart. For the former, both BEM and FEM meshes are drawn. The BEM mesh has 331 nodes and 165 elements, the FEM mesh has 1627 nodes and 730 elements, and the open setup in BEM has 238 nodes and 118 elements. The mesh densities for open and closed microphones are very similar. Note that the membrane of the open microphone has some visible thickness and it is surrounded by a ring. These features are not relevant for the results and help defining it with two separate bodies.

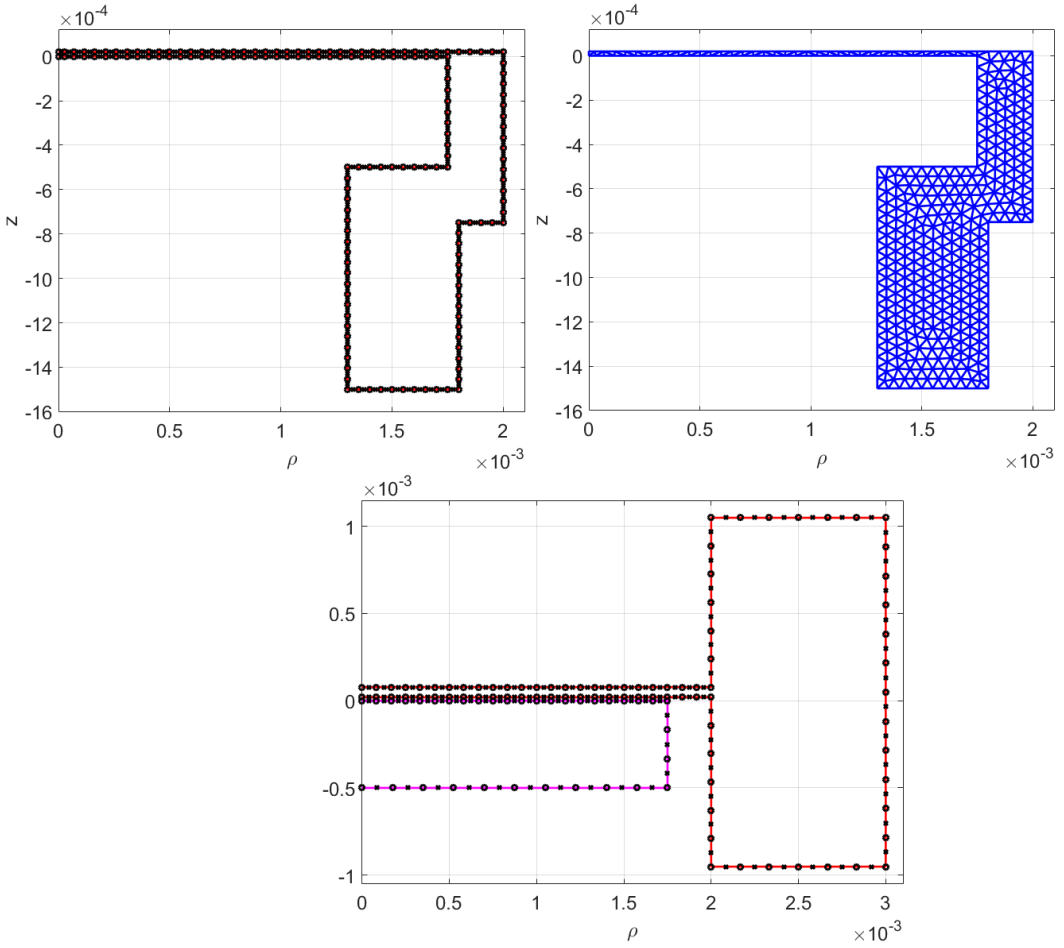

Figure 4: Generator and meshes of the axisymmetrical geometry of the Brüel & Kjær 4938 and its open version. Top left: BEM mesh; top right: FEM mesh; bottom: open microphone version. The excitation is a uniform pressure on the membrane.

The analytical sound pressure in the back cavity represented in Figure 5 is calculated by assuming that the pressure is uniform and the cavity behaves as a compliance, which is valid for low frequencies. The velocity of the membrane exciting the cavity's compliance is also calculated analytically according to [17]. This analytical interior pressure is compared with the calculated pressure using the BEM and FEM-BEM formulations. Neither model gets close to the low-frequency value, but again the FEM-BEM performs slightly better.

Figure 6 represents the calculated microphone sensitivity of the three calculations against the bounds in the actuator measurements. Here it is interesting to observe that the open microphone gives an excellent result. The open microphone is not affected by the low-frequency interior domain issue. The FEM-BEM and the BEM formulations for the original Brüel & Kjær 4938 show sensitivity drops at low frequencies, with again the FEM-BEM performing slightly better.

Finally, Figure 7 shows the condition numbers of the $\mathbf{A}_a$ matrix in Eq. (8) for the closed and open microphones. This result indicates that the closed cavity provokes a loss of accuracy and increased instability as the frequency becomes lower, but this efect is absent when the cavity is opened.

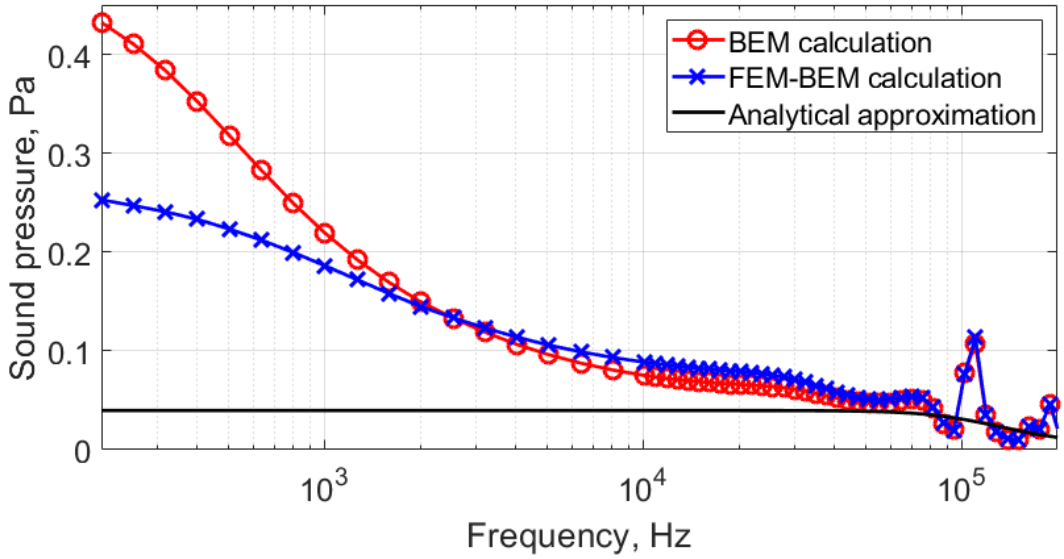

Figure 5: Sound pressure modulus at the bottom of the back cavity of the Brüel & Kjær 4938 microphone. Circles: BEM-only calculation; crosses: FEM-BEM calculation; solid line: Low-frequency analytical approximation based on [17].

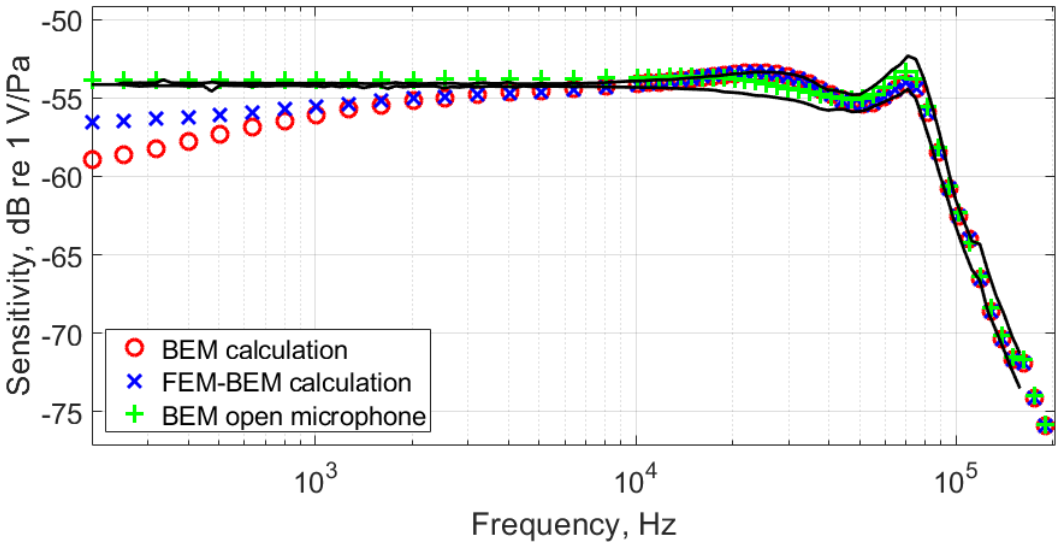

Figure 6: Microphone sensitivity of the Brüel & Kjær 4938 microphone. Circles: BEM-only calculation; crosses: FEM-BEM calculation; pluses: open microphone with the same gap, membrane and back plate dimensions. The solid lines indicate the lower and upper bounds of sensitivity measurements on 183 units of this microphone type.

6. CONCLUSIONS

The low-frequency instability issue described in this paper clearly shows in the examples presented. A new numerical formulation with visco-thermal losses that is a combination of FEM and BEM is used to evaluate whether the BEM alone is more affected by this difficulty. It is shown that even with a FEM model of the propagating acoustic part of the sound fiend, the instability shows at low frequencies. An open microphone is not affected by the issue. The combination of modeling losses, the narrow gap, the uniform interior pressure and the closed cavity makes the solution drift away

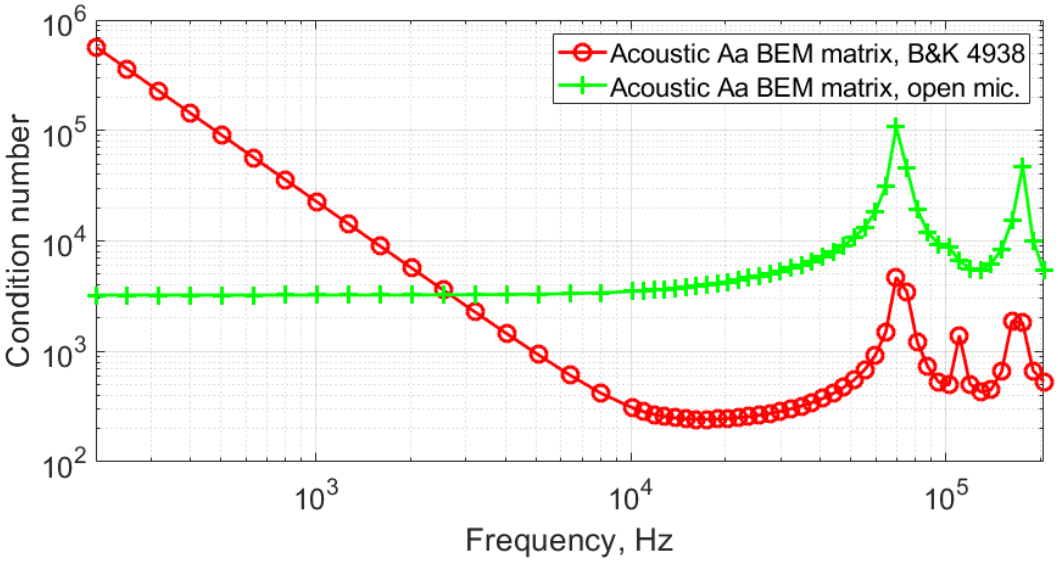

Figure 7: Condition numbers of the acoustic coefficient matrix $\mathbf{A}_a$ in Eq. (8). Circles: Brüel & Kjær 4938 model; crosses: Open version of the microphone.

from the true value. Full FEM models in the literature do not seem to be affected by this issue, possibly because the viscous and thermal boundary layers are meshed in detail, while BEM with losses does not require such meshing, thus saving computational load.

The FEM-BEM formulation, while not a complete remedy for the issue examined here, seems to be promising because its coefficient matrices are sparse and easier to solve.

7. ACKNOWLEDGEMENTS

The authors acknowledge Brüel & Kjær for the information about the type 4938 microphone.

REFERENCES

[1] D. Homentcovschi and R. N. Miles. An analytical-numerical method for determining the mechanical response of a condenser microphone. *Journal of the Acoustical Society of America*, 130(6):3698–3705, 2011.

[2] M.J.H. Jensen and E.S. Olsen. Virtual prototyping of condenser microphones using the finite element method for detailed electric, mechanic, and acoustic characterization. In *ICA 2013 Montreal, Canada, 2-7 June 2013, Proceedings of Meetings on Acoustics, Vol. 19, 030039 (2013)*, 2013.

[3] V. Cutanda Henríquez and P.M. Juhl. An axisymmetric boundary element formulation of sound wave propagation in fluids including viscous and thermal losses. *Journal of the Acoustical Society of America*, 134(5):3409, 2013.

[4] V. Cutanda Henríquez and P. M. Juhl. Implementation of an acoustic 3D BEM with visco-thermal losses. In *Proc. Internoise 2013, 15–18 September 2013, Innsbruck, Austria*, 2013.

[5] V. Cutanda Henríquez and P. M. Juhl. Modelling measurement microphones using BEM with visco-thermal losses. In *Proc. Joint Baltic-Nordic Acoustics Meeting, 18–20 June 2012, Odense, Denmark*, 2012.

[6] V. Cutanda Henríquez, S. Barrera Figueroa, and P. M. Juhl. Study of the acoustical properties of a condenser microphone under an obliquely incident plane wave using a fully coupled three-dimensional numerical model. In *Proc. Internoise 2015, 9–12 August 2015, San Francisco, USA*, 2015.

[7] S. Sorokin and S.T. Christensen. Low-frequency breakdown of boundary element formulation for closed cavities in excitation conditions with 'breathing'-type component. *Communications in Numerical Methods in Engineering*, 16(5):325–334, 2000.

[8] K.A. Hussain and K.S. Peat. Boundary element analysis of low frequency cavity acoustical problems. *Journal of Sound and Vibration*, 169(2):197–209, 1994.

[9] V. Cutanda Henríquez and P. M. Juhl. Implementation aspects of the Boundary Element Method including viscous and thermal losses. In *Proc. Internoise 2014, 16-19 November 2014, Melbourne, Australia*, 2014.

[10] V. Cutanda Henríquez and P. Risby Andersen. A three-dimensional acoustic Boundary Element Method formulation with viscous and thermal losses based on shape function derivatives. *Journal of Computational Acoustics*, 26(3):1859939, 2018.

[11] P. Risby Andersen, V. Cutanda Henríquez, N. Aage, and S. Marburg. A two-dimensional acoustic tangential derivative Boundary Element Method including viscous and thermal losses. *Journal of Computational Acoustics*, 26(3):1850036, 2018.

[12] V. Cutanda Henríquez and P. M. Juhl. Openbem — an open source Boundary Element Method software in acoustics. In *Proc. Internoise 2010, 13–16 June 2010, Lisbon, Portugal*, 2010.

[13] P.M. Juhl. *The Boundary Element Method for sound field calculations*. Ph.D. thesis, Report No. 55, Technical University of Denmark, 1993.

[14] A.D. Pierce. *Acoustics: An Introduction to Its Physical Principles and Applications, Chap. 10*. McGraw Hill, New York, 1981.

[15] M. Bruneau, Ph. Herzog, J. Kergomard, and J. D. Polack. General formulation of the dispersion equation in bounded visco-thermal fluid, and application to some simple geometries. *Wave Motion 11*, page 441–451, 1989.

[16] G. Plantier and M. Bruneau. Heat conduction effects on the acoustic response of a membrane separated by a very thin air film from a backing electrode. *Journal d'Acoustique*, 3(3):246–250, 1990.

[17] G.S.K. Wong and T.F.W. Embleton. *The AIP Handbook of Condenser Microphones. Theory, Calibration, and Measurements (Ch. 3)*. American Institute of Physics, 1995.